Journal of Nepal Geological Society, 2001, Vol. 23, pp. 99–110

Geo-hydrological hazard and risk zonation of Banganga watershed using GIS and remote sensing

Motilal Ghimire
Central Department of Geography, Tribhuvan University, Kirtipur, Kathmandu, Nepal

ABSTRACT

The present study attempts to analyse the terrain elements and geo-hydrological processes operating on the Banganga watershed in western Nepal. The paper also assesses the hazard and risk to the land use, land cover, and settlements. The Banganga watershed is highly rugged, steep, and fragile. Based on GIS, a geo-hydrological hazard map, a vulnerability map, and a risk map were prepared. In the study area, the geo-hydrological processes are active and intense during the monsoon season. Instabilities are generally found on steep slopes with high relative relief, in areas underlain by the Siwaliks, and along the fault zones. The mass movements are more frequent on slopes covered by dense to moderately dense forest than on the agricultural land. The socio-economic significance of the hazard in the watershed is considerably high. About 8% of the agricultural land lies in the very high and high hazard zones. Similarly, 18 houses are located in the very hazard zone, 93 houses in the high hazard zone, 211 in the moderately high hazard zone, and the rest of 2,185 houses in the moderate and low hazard zones. The risk map generated by combining the hazard map and vulnerability map shows 14% of the area under the very high and high risk zones, 38% under the moderate risk zone, and 48% under the low risk zone.

INTRODUCTION

The Banganga watershed (Fig. 1) lies in the Siwaliks and the Middle Mountains of the Lumbini Zone in western Nepal. It lies between latitudes 27° 41' 30" and 27° 54' 07" N, and longitudes 80° 04' 22" and 80° 18' 56" E in the hills of the Western Development Region with the total area of 207 km^2.

Steep slope, high river gradient, predominance of fragile rock, and high seismicity make the watershed highly susceptible to erosion and landslides. Prolonged and high-intensity rains in the monsoon season are also the most important factors triggering mass movements (Starkel 1972; Dhital et al. 1993). Landform, lithology, rock structure, hydrology, seismicity, and land use are the most important terrain elements that determine the nature and intensity of the geo-hydrological processes (Verstappen 1983; Deoja et al. 1991; Van Westen 1993; Mehrotra et al. 1996). Considering the above facts, the present study aims at analysing the terrain elements and the geo-hydrological processes in order to generate geo-hydrological hazard and risk zonation maps of the watershed.

The term *landslide* is generally used to denote the downward and outward movement of slope-forming materials along surfaces of separation (Varnes 1984). In this paper, it is used in a broader context to include true sliding as well as falls and earth flows. The terms *hazard*, *vulnerability*, and *risk* are defined as follows (Varnes 1984; UNDRO 1991):

Hazard (H) means the probability of occurrence, within the specified period of time and within a given area, of a potentially damaging phenomenon.

The term *geo-hydrological hazard* is used here to indicate hazards resulting from the catastrophic geomorphic events such as landslides, gully erosion, bank cutting, river channel shifting, and flooding.

Vulnerability (V) means the degree or loss to given element or set of elements at risk resulting from the occurrence of a natural phenomenon of a given magnitude.

Risk (R) can be defined as the expected degree of loss due to a particular natural phenomenon.

GEOLOGY AND PHYSIOGRAPHY

The Siwaliks of Neogene age occupy the southern half of the watershed (Fig. 2) and they are further subdivided into the Lower Siwaliks (interbedded variegated mudstone and grey-green sandstone), Middle Siwaliks (up to 25 m thick beds of grey sandstone and dark grey mudstone), and Upper Siwaliks (Grey and brown conglomerate and mudstone). The Siwaliks are delimited in the north by the Main Boundary Thrust (MBT) and the remaining area is made up of the Precambrian to Eocene Lesser Himalayan rocks (Fig. 2). The latter comprise slate, shale, limestone, dolomite, sandstone, and quartzite. Besides the MBT, there are also other several essentially northwest–southeast trending major faults and some minor faults. The Mahabharat Range is essentially parallel to the MBT.

The Banganga basin is elongated in shape (Fig. 1) and its average relief is 830 m as against the minimum and maximum values of 125 and 2,250 m, respectively. The average slope of the basin above its outlet is 28°. The hypsometric

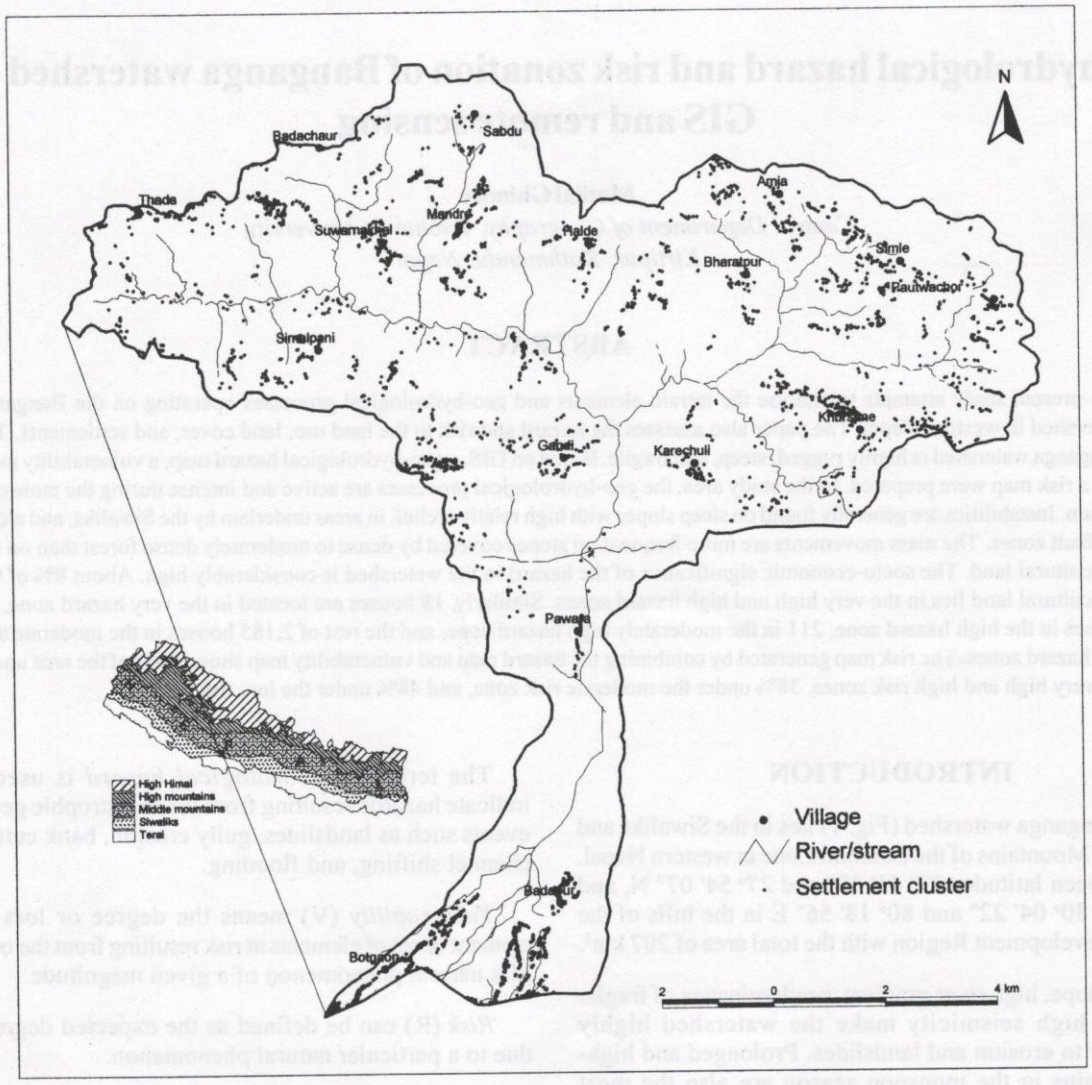

Fig. 1: Location of the Banganga watershed

curve analysis shows the steep and rugged terrain above 1,400 m as well as between 200 and 600 m, moderately gentle slope between 600 and 1,400, and gentle slope below 200 m.

The Banganga and Dhungre Rivers drain the watershed and their mean gradient is 5.7 and 6.7°, respectively. The overall drainage density is 3.8 km/km^2. The drainage pattern is dendritic on the Lesser Himalayan rocks and it is trellis on the Siwaliks.

The altitudinal variation has led to the climatic changes in the study area. From an altitude of about 1,500 m, the climate changes from subtropical (with the deciduous forest) to warm temperate type. The mean daily temperature ranges from less than 9.5 (January) to 20.5 °C (July) in the higher altitudes and from 17 (January) to 30.5 °C (July) in the lower altitudes. The mean annual precipitation in the basin ranges from about 1,818 mm in the northern part to 2,520 mm in the southern part. More than 88% of the total rain occurs during the summer monsoon (i.e. between June and September).

SOCIO-ECONOMIC CONDITIONS

The estimated households in the Banganga watershed are 3,969 and they spread over 41 settlements. The distribution of population is uneven and is dictated mainly by the agriculture potential of the terrain mostly determined by the slope and soil depth. The mainstay of the people is agriculture (92%). Labour and foreign remittance are the two main income sources. The level of food availability in the entire region is very low. Only 26% of households produce the food on a subsistence level. The food availability situation is particularly worse in hills.

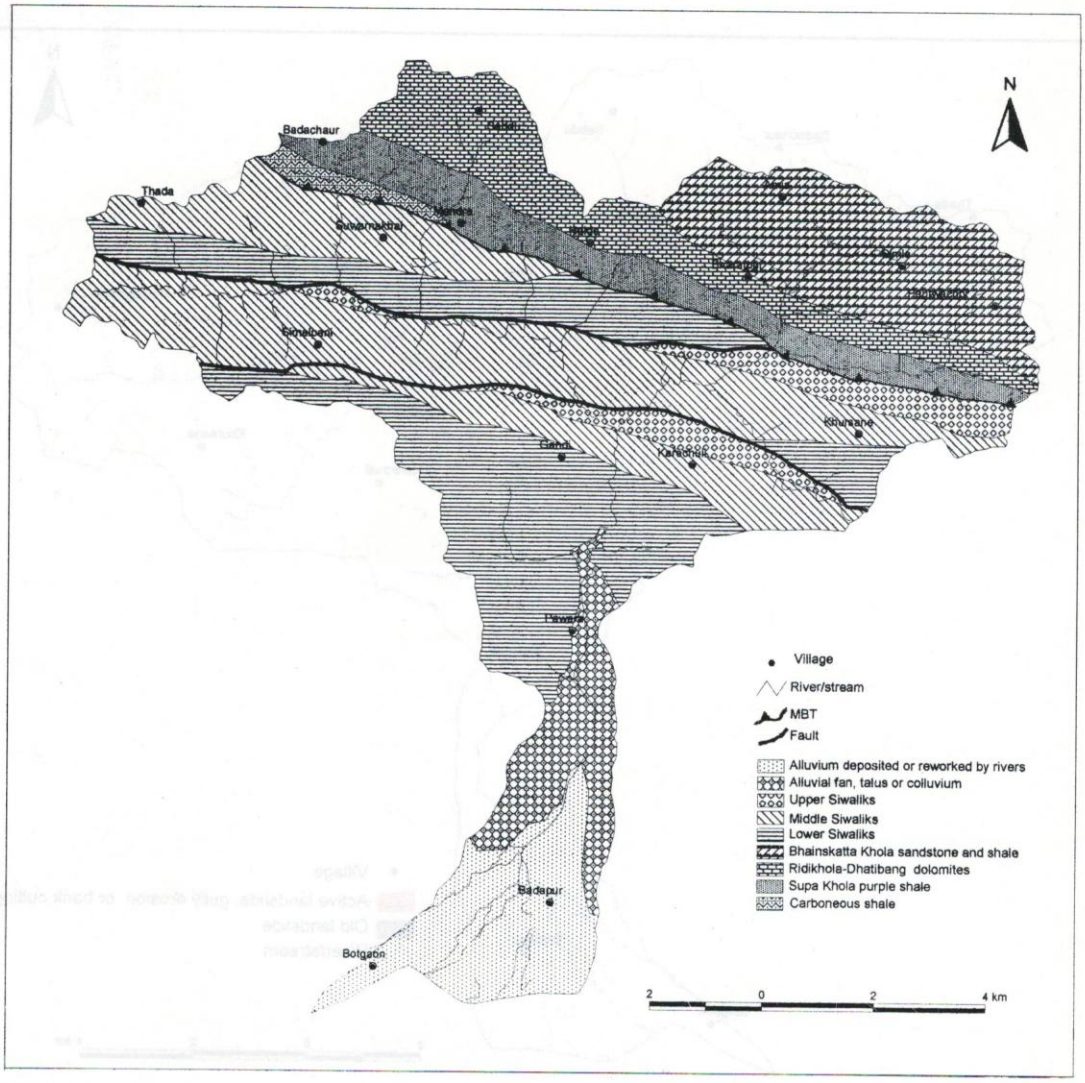

Fig. 2: Geological map of the Banganga watershed

GEO-HYDROLOGICAL PROCESSES

In the present study, the geo-hydrological processes are categorised into 1) landslides; 2) gully erosion, riverbank erosion, and channel shifting; and 3) floods (Fig. 3). A brief discussion of each of them is given below.

Landslides

About 110 active landslides were identified from the satellite imagery and aerial photographs, which were later verified and updated in the field (Fig. 3). The spatial landslide distribution pattern based on the Point Pattern Analysis technique (Boots and Gettis 1988) indicated the clustered type rather than the regular or random type. The probability of occurrence of a new landslide within the distance of 5 km from any existing landslide is about 0.5. The length of landslide (including the area occupied by displaced mass) varies from 10 to 400 m with an average length of 110 m and width varies from 250 m with an average of 54 m. Similarly, the depth of landslide varies from 0.3 to 20 m with an average of 4 m. Thus, there is a significant variation in the landslide dimensions.

Landslide density

Generally, convex slopes are more stable as they disperse the runoff more equally down the slope and concave slopes as potentially unstable as they concentrate water at the lowest point and contribute to the built up of adverse hydrostatic pressure (Stocking 1972). Contrary to it, the convex slopes in the study area (Table 1) have the highest landslide density (i.e. 0.067) and the straight slopes have the lowest density (i.e. 0.0027). Most landslides on convex slopes were found on the Siwaliks. The landslides on convex slopes are of mixed to rotational types without distinct planes of failure. At places, they are associated with soil creep, especially on the upper slopes.

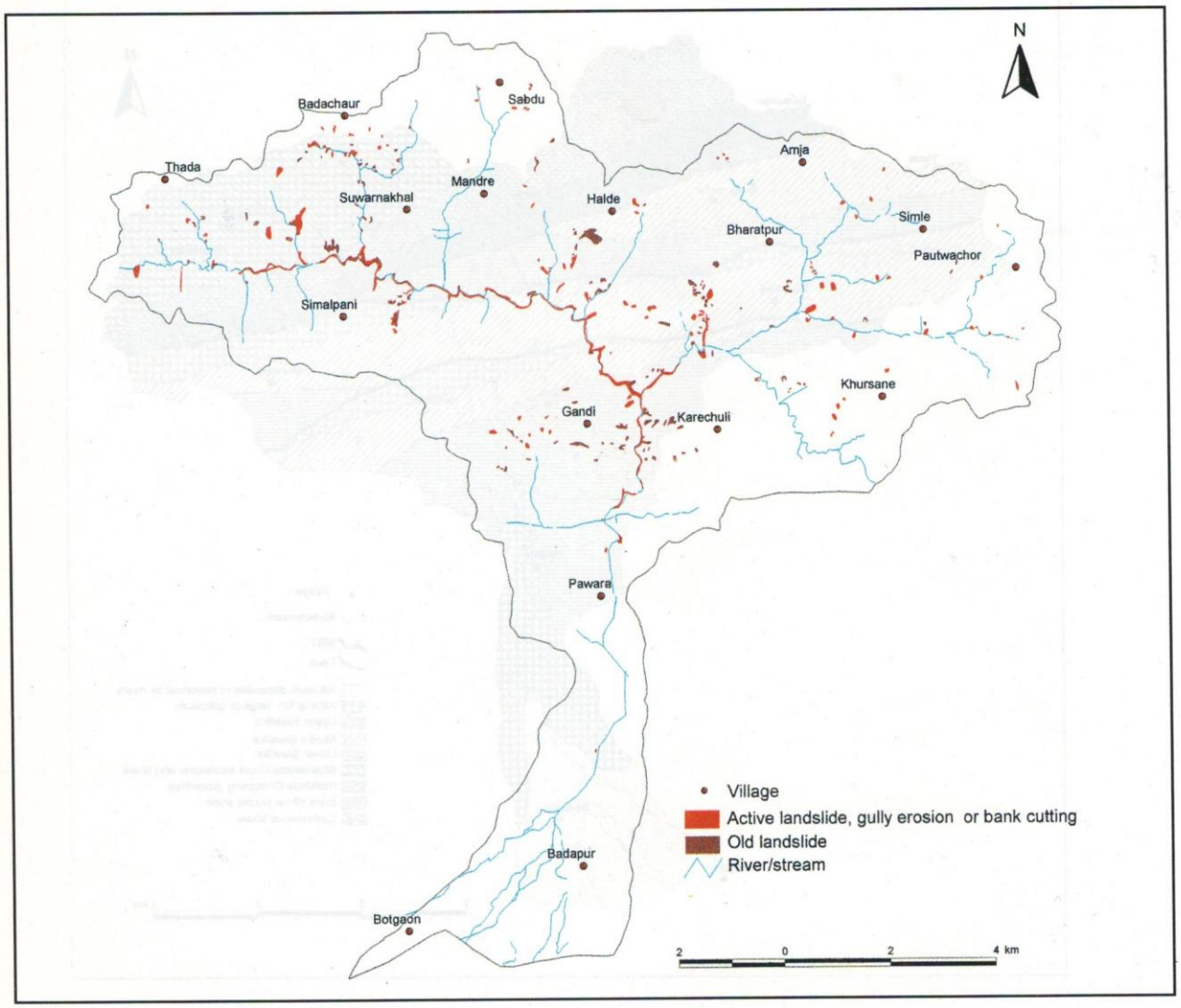

Fig. 3: Map of geo-hydrological processes in the Banganga watershed

About 53% of the area is steeper than 25° (Fig. 4; Table 1). The landslide density increases with the slope gradient (r = 0.924). However, some previous studies (Deoja et al. 1991) indicated that the highest landslide density was on the slope interval of 25–35° whereas the steeper slopes had a lower density. The reason for high landslide density on the steeper slopes of the Banganga watershed is the reactivation of the old and steep landslide scars, the presence of more than three sets of joint in the bedrock, and the formation of perched aquifers exerting high pore water pressure.

Similarly, the relative relief indicates the potential energy for erosion and mass wasting. The relative relief varies from less than 25 to above 75 m within the area of 1 ha. Notably, 52% of the area lies within 0–25 m of relative relief and only about 4.67% lies above 50 m. There is a strong correlation between the relative relief and landslide density (Table 2).

The landslide density is high in black and carbonaceous shales (Fig. 2; Table 2) owing to their cleaved nature and high rate of weathering. Such rocks are predominant on the middle slopes of the Mahabharat Range. Similarly, the Lower and Middle Siwalik shales also exhibit a significantly high landslide density (Table 2).

About 38 lineaments (with the total length of 99 km) representing faults and major joints were detected in the study area. The landslide density has a direct relationship with the distance from the lineaments (Table 2). There is a strong positive correlation (r=0.96) between the landslide density and the proximity of a lineament. The highest density is found within the distance of 60 m from the lineaments. This suggests that the geological discontinuities have significantly contributed in triggering landslides.

Table 1: Relationship between topographic elements and landslide density

Category	No. of pixels (10x10 m^2)		Landslide density	Weight
	Landslide	Parameter class		
Slope shape				
Concave	2,114	345,051	0.0061	0.4473
Convex	2,285	341,807	0.0067	0.5411
Straight	3,663	1,360,854	0.0027	-0.3677
Slope gradient (°)				
Gentle (0–7)	277	332,202	0.0008	-1.5841
Moderately sloping (7–15)	479	181,308	0.0026	-0.4055
Moderately steep(15–25)	1,287	445,324	0.0029	-0.2963
Steep(25–35)	2,306	565,870	0.0041	0.05
Strongly steep(35–45)	2,559	422,092	0.0061	0.4473
Cliff/escarpment(>45)	1,154	107,945	0.0107	1.0093
Relative relief (m)				
Low (<400)	355,010	213	0.0006	-1.8718
Moderately low (400–800)	476,648	2,670	0.0056	0.3618
Moderate (800–1,200)	750,656	4,428	0.0059	0.414
Moderately high (1,200–1,600)	361,407	725	0.002	-0.6678
High (>1,600)	129,615	26	0.0002	-2.9704
Relative relief (m)				
Low (0–25)	2,101	1,076,909	0.002	-0.6678
Moderate (25–50)	5,035	896,647	0.0056	0.3618
Moderately high (50–75)	812	69,354	0.0117	1.0986
High (>75)	114	5,661	0.0201	1.6397

Source: GIS (ILWIS 2.1)-based DTM generated from topographic maps of 1993, satellite image interpretation, and ground truth 1999

Table 2: Relationship between geology and landslide density

Category	Number of pixels (10 m)		Landslide density	Weight
	Landslide	Parameter class		
Rock or soil type				
Alluvial fan, talus, and colluvium	125	113,320	0.0011	-1.2657
Alluvium deposited or reworked by rivers	7	174,485	0.0001	-3.6636
Upper Siwaliks	346	109,166	0.0032	-0.1978
Middle Siwaliks	2,632	570,735	0.0046	0.1651
Lower Siwaliks	2,391	488,267	0.0049	0.2283
Bhainskatta Khola sandstone and shale	447	242,429	0.0018	-0.7732
Black and carbonaceous shale	471	21,468	0.0219	1.7255
Ridikhola–Dhatibang dolomites	742	193,245	0.0038	-0.026
Supa Khola purple shale	901	160,203	0.0056	0.3618
Distance from lineament (m)				
Near (0–39)	66,633	553	0.0083	0.7553
Moderately near (30-60)	58,004	491	0.0085	0.7791
Moderate (60–90)	60,150	442	0.0073	0.6269
Moderately far (90–120)	61,169	400	0.0065	0.5108
Far (120–200)	164,854	808	0.0049	0.2283
Very far (> 200)	1,660,707	5,350	0.0032	-0.1978
Dip slope relationship				
Counter dip slope	4,243	1,099,055	0.0039	0
Dip slope	2,054	556,066	0.0037	-0.0526
Perpendicular to dip direction	1,765	417,408	0.0042	0.0741

Source: Geological map (Aryal 1978), satellite image interpretation, and ground truth 1999

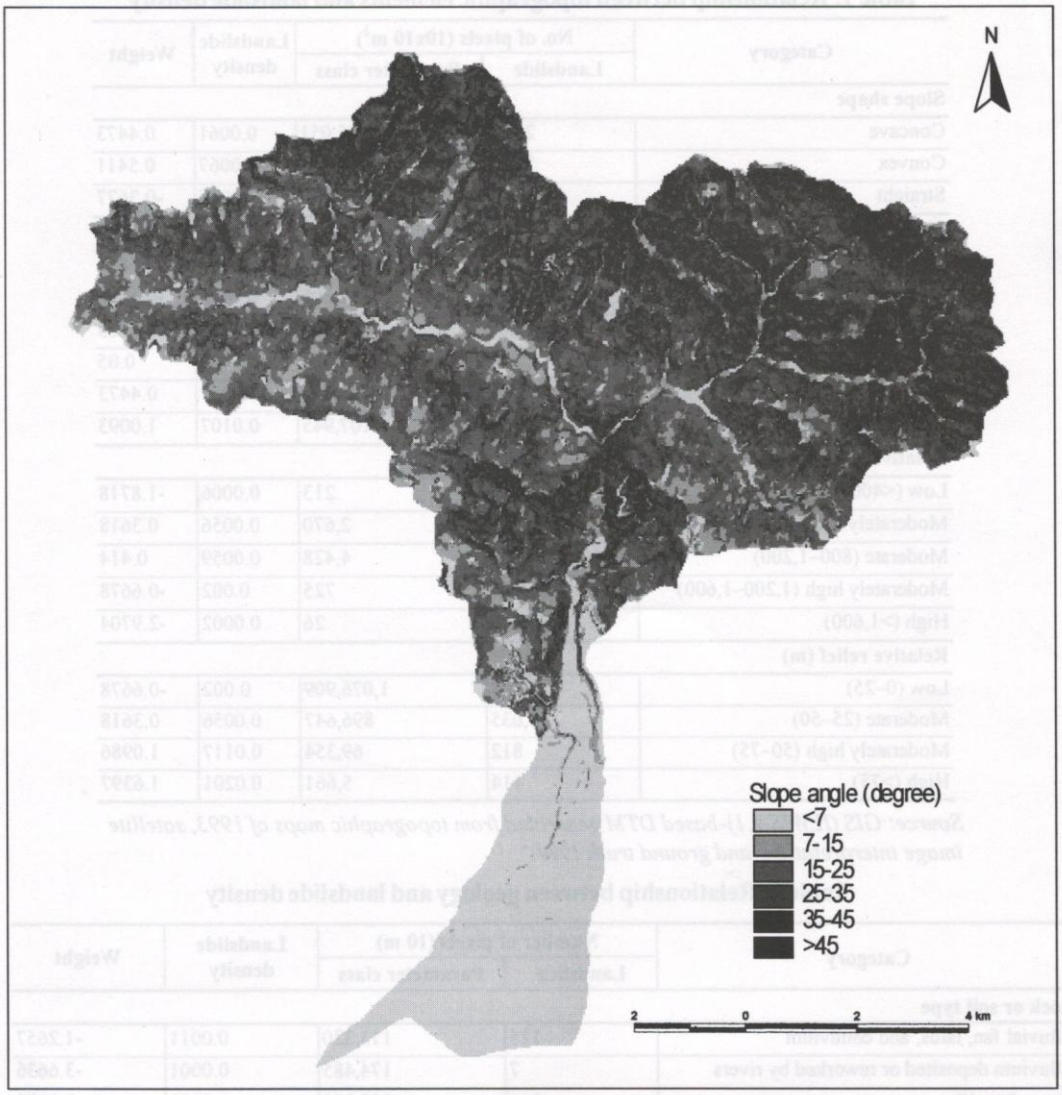

Fig. 4: Slope map of the Banganga watershed

The dip slope plays an important role in overall slope stability (Verstappen 1983). On the dip slope, potential zones of weakness and failure surfaces are prominent. Additionally, the dip slopes tend to concentrate subsurface water and return it to the surface. Table 2 shows the highest landslide density on slopes perpendicular to bedding and the lowest on the dip slopes. It is probably related to the presence of prominent joints in the direction perpendicular or oblique to the bedding.

Forest and cultivated land occupy respectively 70 and 24% of the Banganga watershed. The study of land use and land cover (Fig. 5) has shown a maximum landslide density on rock and soil cliffs (Table 3). The landslide density in the forest and cultivated land is 0.0044 and 0.0025, respectively. The slopes with moderate to moderately high vegetation cover have the highest landslide density (Table 3).

Gully erosion, riverbank erosion, and channel shifting

The active gullies, bank erosion scars, and abandoned channels were identified mainly from the imagery and they were further verified in the field. The gully is a rapid erosional feature and it may evolve from a wide and deep rill (Selby 1993). The gullies with or without a head scarp were identified in the study area. The gullies with head scarps are widespread mainly on brittle shales of the Pakri–Jaluke region. The gullies without head scarps commonly develop on highly weathered rock or colluvium as a result of gradual expansion of rills. Such gullies are common on the Siwaliks and the concave slopes of the Lesser Himalaya. They become natural drainage lines of surface runoff during the monsoon.

Bank erosion is extensive along the Banganga River, especially between Botgaon and the confluence of the Bahune Khola (Fig. 2). But the lateral extent of bank erosion

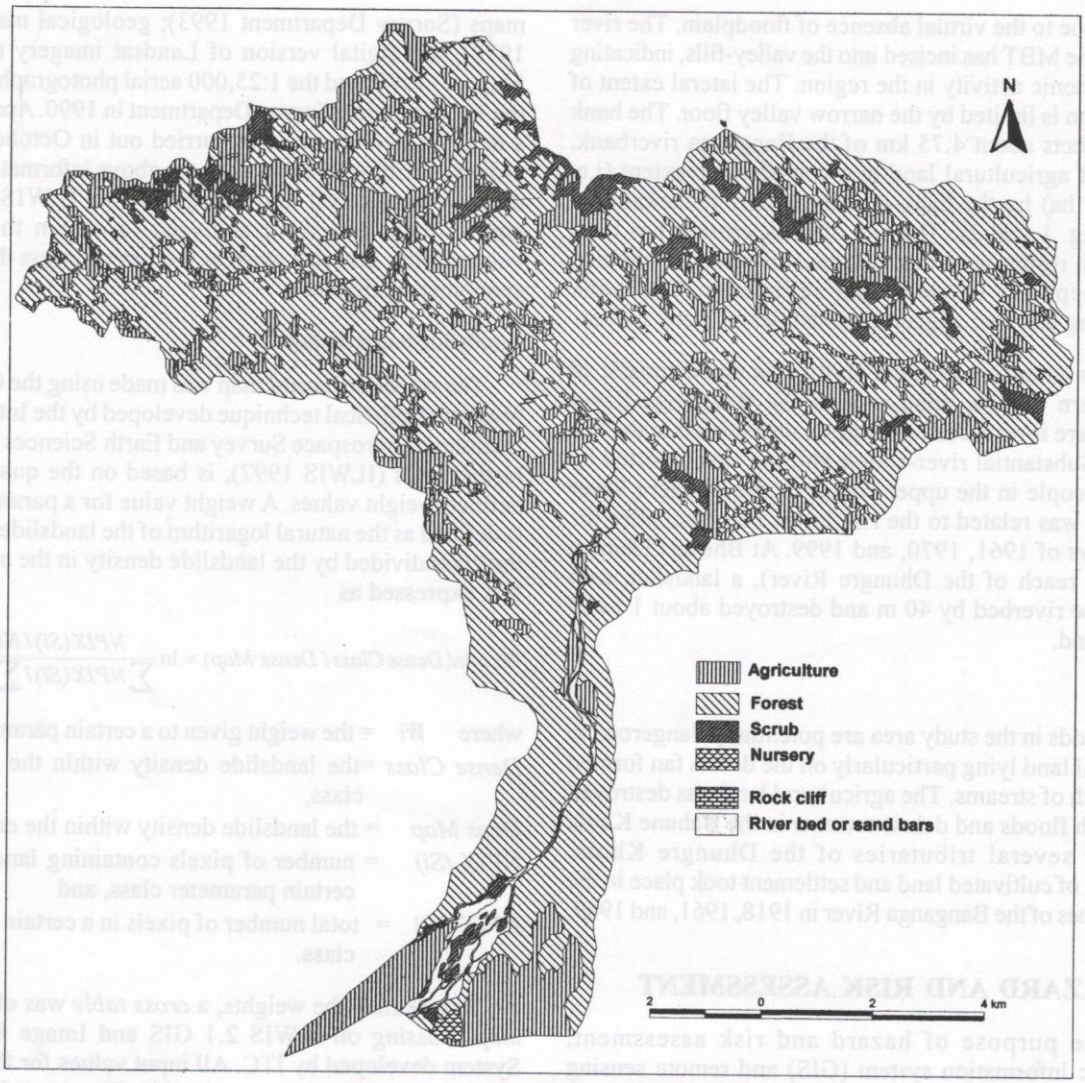

Fig. 5: Land use and land cover map of the Banganga watershed

Table 3: Relationship between land use/land cover and landslide density

Land use/land cover	No of pixels		Landslide density	Weight
	Active slide	Parameter class		
Agriculture	1,195	487,327	0.0025	-0.4447
Forest	6,467	1,459,631	0.0044	0.1206
Nursery	0	3,590	0.00001	-5.9661
Rock cliff	92	3,189	0.0288	1.9994
Sand deposits and riverbed	0	34,094	0.0005	-7.66429
Scrub	292	83,832	0.0035	-0.1082
Total	**8,062**	**2,071,663**	**0.0039**	
Vegetation density class				
High density	2,188	738,485	0.0030	-0.2624
Moderately high density	2,118	489,419	0.0043	0.0976
Moderate density	3,168	560,398	0.0057	0.3795
Low density	588	284,326	0.0021	-0.619
Total	**8,062**	**2,072,628**	**0.0039**	

Source: Aerial photographs of 1990; topographic maps of 1993 at 1:25,000; Normalised Density of Vegetation Index obtained from digital image processing and ground truth

is limited due to the virtual absence of floodplain. The river following the MBT has incised into the valley-fills, indicating the neo-tectonic activity in the region. The lateral extent of bank erosion is limited by the narrow valley floor. The bank erosion affects about 4.75 km of the Banganga riverbank. The loss of agricultural land in a considerable extent (i.e. about 1.45 ha) by the bank erosion is only remarkable at Pawara (Fig. 1 and 2). The site of bank erosion has been changing in response to the dynamics of meander position and the deposits of reworked sediments. The bank undercutting has also triggered landslides in many places.

Though extensive channel shifting is characteristic of the southern narrow zone around the Banganga River (Fig. 3), there is no record of large-scale avulsion in the last 40 years. Substantial river-course shifting was reported by the local people in the upper course of the Dhungre River (Fig. 1). It was related to the rise in the bed level after the debris flows of 1961, 1970, and 1999. At Bhakari Dhunga (the upper reach of the Dhungre River), a landslide dam diverted the riverbed by 40 m and destroyed about 1 ha of irrigated land.

Floods

The floods in the study area are potentially dangerous to agricultural land lying particularly on the debris fan formed at the mouth of streams. The agricultural land was destroyed by the flash floods and debris torrents in the Bahune Khola and other several tributaries of the Dhungre Khola. Inundation of cultivated land and settlement took place in the lower reaches of the Banganga River in 1918, 1961, and 1969.

HAZARD AND RISK ASSESSMENT

For the purpose of hazard and risk assessment, geographic information system (GIS) and remote sensing were used to prepare various spatial data layers (Table 4). These data were obtained from the 1:25,000 scale topographic maps (Survey Department 1993); geological maps (Aryal 1978), the digital version of Landsat imagery (Thematic Mapper) 1998; and the 1:25,000 aerial photographs taken by the Topographical Survey Department in 1990. Apart from it, a detailed field survey was carried out in October 1999 in order to verify, edit, and update the above information. These data were entered and integrated in ILWIS 2.1 GIS environment and were analysed to obtain the hazard, vulnerability, and risk maps as well as to assess their socio-economic significance.

Landslide hazard map

The landslide hazard map was made using the GIS-based bivariate statistical technique developed by the International Institute of Aerospace Survey and Earth Sciences (ITC), the Netherlands (ILWIS 1997), is based on the quantitatively defined weight values. A weight value for a parameter class is defined as the natural logarithm of the landslide density in the class divided by the landslide density in the entire map. It is expressed as

$$Wi = \ln(Dense\,Class / Dense\,Map) = \ln \frac{NPIX(Si)/NPIX(Ni)}{\sum NPIX(Si)/\sum NPIX(Ni)}$$

where Wi = the weight given to a certain parameter class,
Dense Class = the landslide density within the parameter class,
Dens Map = the landslide density within the entire map,
NPI*X (Si)* = number of pixels containing landslide in a certain parameter class, and
NPIX (Ni) = total number of pixels in a certain parameter class.

To calculate the weights, a *cross table* was obtained by *map crossing* on ILWIS 2.1 GIS and Image Processing System developed by ITC. All input values for the formula were obtained from the *cross table*. The natural logarithm was used to give a negative weight when the landslide

Table 4: Types of data layer and their method of generation

Data layer	Database	Parameters	Method of generation
Geology	Geological map	Rock type	GIS
Structure	Geological map and Landsat (TM)	Lineaments and dip slope relationship	VI/FC and GIS
Topography	Topographic maps	Slope gradient, slope shape, and relative relief	GIS-based digital elevation model
Hydrology	Topographic maps and aerial photographs	River and channel bed	VI/FC and GIS
Geomorphic Process map	Topographic maps and aerial photographs	Landslide, gully erosion, and channel shifting	VI/FC and GIS
Vegetation density	Landsat (TM) 1998	Density class	Digital image processing (DIP)
Land use/land cover	Aerial photographs and Landsat (TM) 1998	Land use and land cover types	VI/FC, DIP, and GIS
Settlement	Topographic maps and aerial photographs	Location of houses and population density	VI/FC and GIS

VI: Visual interpretation of Aerial photo/Imagery, FC: Field check

density was lower than the normal, and a positive weight when it was higher than the normal. The following maps were combined to obtain the landslide hazard map:

- Weight map of slope shape,
- Weight map of slope gradient,
- Weight map of relative relief,
- Weight map of geology,
- Weight map of geomorphology,
- Weight map of dip slope relationship,
- Weight map of lineament distance,
- Weight map of vegetation density, and
- Weight map of land use.

Geo-hydrological hazard map

The geo-hydrological hazard map (Fig. 2) was prepared by combining the landslide hazard map with the following geo-hydrological hazards: gully erosion, inundation, bank erosion, and river channel shifting.

About 26% of the area lies in the very high and high hazard zones (which contain about 73% of active landslides) and about 42% of the territory lies in the moderate hazard zone. Similarly, about 19 and 12% of the land falls under the moderately low hazard zone and low hazard zone, respectively (Table 5). Most of the area under high and very high hazard lies in the middle reaches of the Banganga River, along the Mandre Khola, and in the Amaja Khola (Fig. 1).

About 54% of the total agricultural land lies in the moderately low and low hazard zones, 38% in the moderate hazard zone, and 8% in the very high and high hazard zones (Table 5; Fig. 6). About 5 and 25% of the forest lies in the very high and high hazard zones, respectively whereas about 45% of the forest falls in the moderate hazard zone (Fig. 7). Only 25% of the forest area lies in the moderately low and low hazard zones.

Location of houses

In the study area, 111 houses (4%) are located in the very high and high hazard zones (Table 6). Out of these, 18 houses are in the sites of eminent hazard. Besides, 211 houses (8%) are located in the moderately high hazard zone. Hence, altogether about 12% of the total houses are located in relatively unsafe areas.

Vulnerability map

The vulnerability map was prepared using the following GIS layers:

- Distance from a house,
- Cultivated land, and
- Population density.

The distance from a house was obtained by *buffering* each house with three distance intervals (i.e. <50, 50–100, and >100 m). The map of cultivated land was extracted from the land use/land cover map. Similarly, the population density of a region in the Banganga watershed was obtained as follows:

$$\text{Population density} = \frac{\text{Number of houses in the region} \times \text{average household size}}{\text{area of the region}}$$

where the average household size of the Lumbini Zone was obtained from CBS (1991).

Then, the vulnerability map was developed as follows:

- Transforming the parameter maps into weight maps by assigning a weight value to each class of the parameter maps;
- Combining various weight maps by adding their corresponding values; and
- Preparing the vulnerability map by classifying the combined weight map into three (i.e. high, medium, and low) classes.

Risk map

Owing to the absence of information on costs and recurrence intervals of geo-hydrological phenomena, the risk map (Fig. 8) was prepared by combining the geo-hydrological hazard map with the vulnerability map.

About 14% of the total area is under the very high and high risk zones in terms of expected loss/damage of property. Similarly, about 38 and 48% of the area is under the moderate risk zone and low-risk zone, respectively. The low risk zone comprises mostly the Terai, ridge tops, arable slopes, cliffs, and settlements.

Table 5: Distribution of land use/land cover in various hazard zones

Hazard zone	Total area		Agriculture		Forest		Scrub		Others	
	ha	%	ha	%	ha	%	ha	%	ha	%
Very high	991.45	4.78	72.52	1.49	729.15	4.99	81.14	9.68	108.64	26.58
High	4,462.88	21.52	323.22	6.63	3,705.4	25.38	180.07	21.48	253.35	61.98
Moderate	8,748.4	42.19	1,865.27	38.25	6,543.14	44.82	339.74	40.53	0.25	0.06
Moderately low	3,948.45	19.04	1,702.31	34.91	2,057.07	14.09	188.53	22.49	0.54	0.13
Low	2,569.6	12.39	911.18	18.69	1,558.84	10.68	48.52	5.79	37.02	9.06
Total	**20,734.41**	**100**	**4,876.17**	**100.00**	**14,596.31**	**99.97**	**838.32**	**100.00**	**408.73**	**100.00**

Source: Hazard map and land use/land cover map

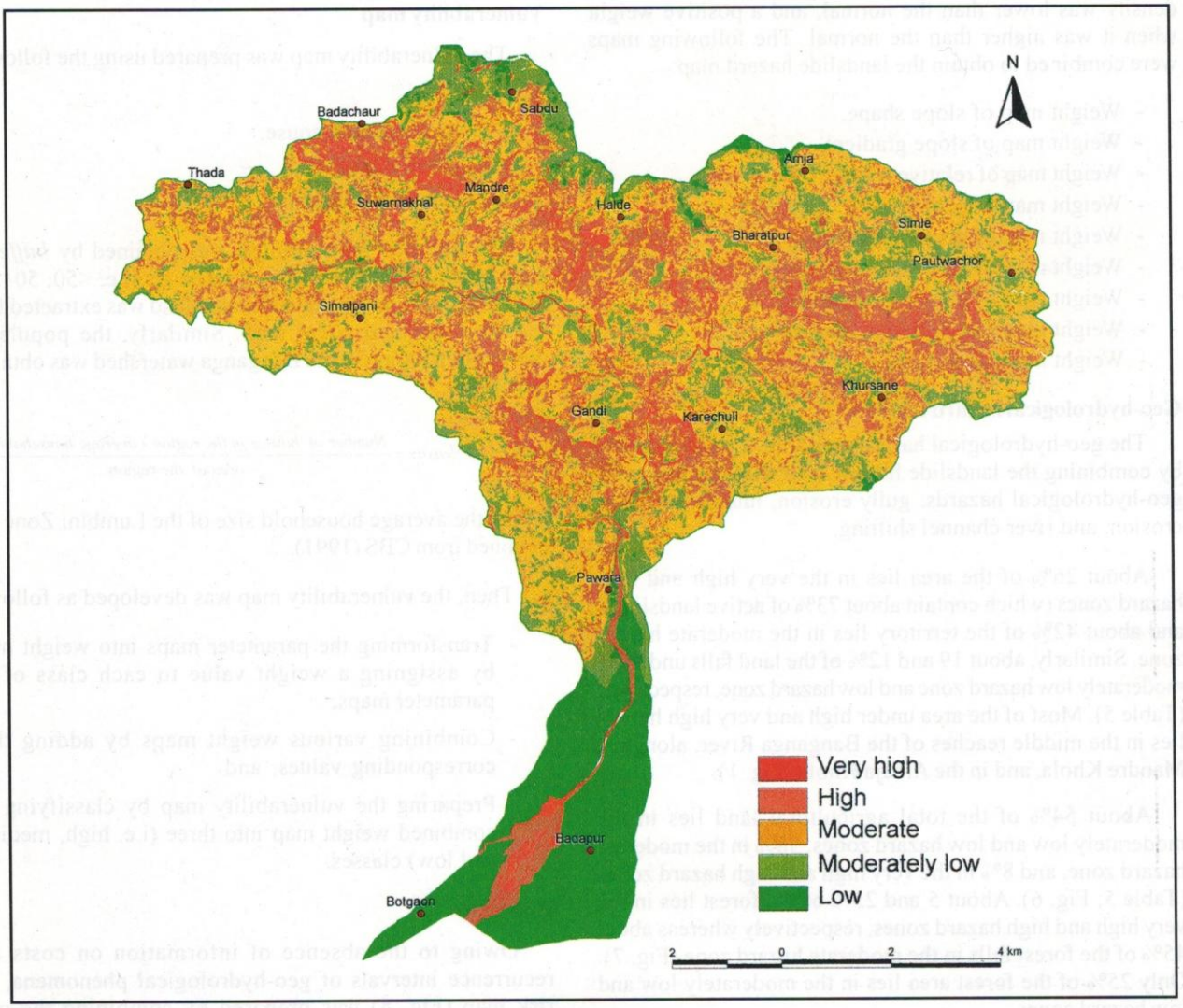

Fig. 6: Geo-hydrological hazard map of the Banganga watershed

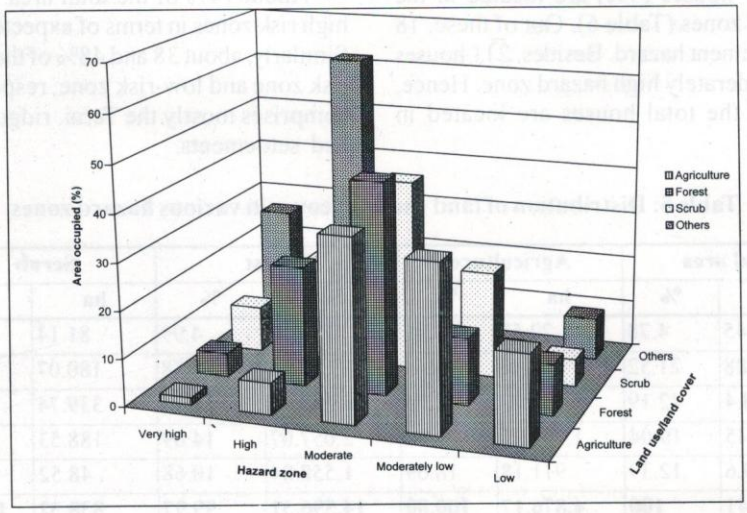

Fig. 7: Relationship between the hazard type and land use/land cover

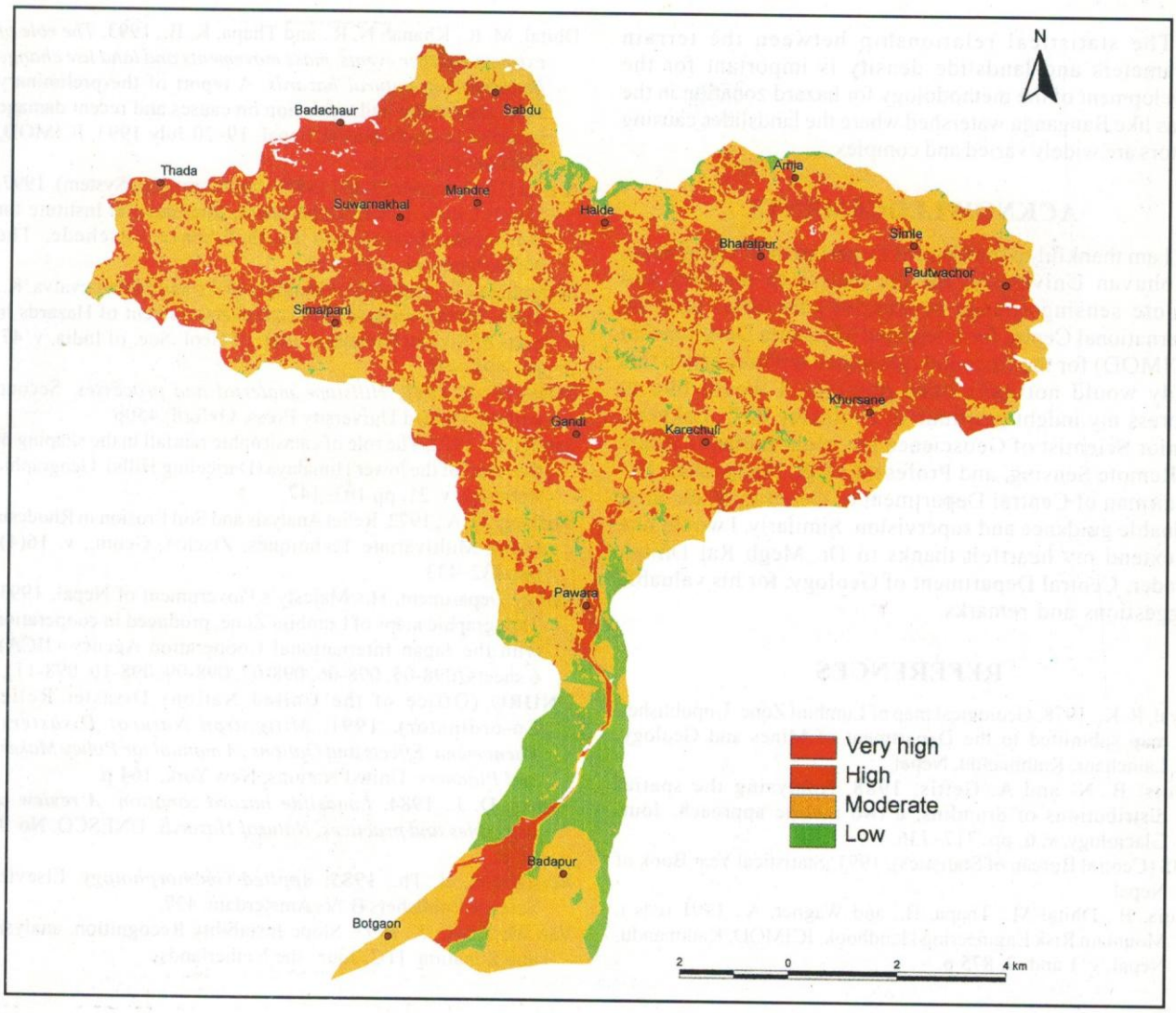

Fig. 8: Risk map of the Banganga watershed

Table 6: Number of houses in various hazard types

Hazard zone	No. of houses	%
Very High	18	0.7
High Hazard	93	3.7
Moderately High	211	8.4
Moderate	1,553	62.0
Low	632	25.2
Total	**2,507**	**100.0**

Source: Hazard map and Field survey

CONCLUSIONS

In the Banganga watershed, the landslides have widely varying dimensions and they are generally clustered. The debris flows raise the bed level and lead to change in the river course at several places in the Dhungre Khola causing damage to the agricultural land. Inundation takes place only during the rare high-magnitude flood events and is limited to the lower fan of the Banganga River.

Potentially unstable slopes are located on slopes with high gradient, high relative relief, in the areas underlain by the Siwaliks and the shale of the Lesser Himalaya. The landslide density is high at the proximity of the fault. They are more frequent on the slopes covered by forest than on the cultivated land. The socio-economic significance of the hazard in the watershed is considerably high. About 8% of the agricultural land falls in the very high and high hazard zones. Similarly, 111 houses are located in the zones of very high and high hazard whereas 211 houses lie in the moderately high hazard zone, and the rest (2,185 houses) lie in the safe areas. About 14% of the territory lies under the very high and high risk zones, 38% under the moderate risk zone, and the rest (48%) under the low risk zone.

The statistical relationship between the terrain parameters and landslide density is important for the development of the methodology for hazard zonation in the areas like Banganga watershed where the landslides causing factors are widely varied and complex.

ACKNOWLEDGEMENTS

I am thankful to the Central Department of Geography, Tribhuvan University, for the access to the GIS and remote sensing (image processing) facilities and the International Centre for Integrated Mountain Development (ICIMOD) for the financial assistance without which this study would not have been possible. I would like to express my indebt gratitude to Professor R. C. Lakhera, Senior Scientist of Geoscience Division, Indian Institute of Remote Sensing, and Professor M. S. Manandhar, Ex-Chairman of Central Department of Geography, for their valuable guidance and supervision. Similarly, I would like to extend my heartfelt thanks to Dr. Megh Raj Dhital, Reader, Central Department of Geology, for his valuable suggestions and remarks.

REFERENCES

Aryal, R. K., 1978, Geological map of Lumbini Zone. Unpublished map submitted to the Department of Mines and Geology, Lainchaur, Kathmandu, Nepal.

Boots, B. N. and A. Gettis, 1988, Analysing the spatial distributions of drumlins: a two mosaic approach. Jour. Glaciology, v. 6, pp. 717–736.

CBS (Central Bureau of Statistics), 1991, Statistical Year Book of Nepal.

Deoja, B., Dhital M., Thapa, B., and Wagner, A., 1991 (eds.), Mountain Risk Engineering Handbook. ICIMOD, Kathmandu, Nepal, v. 1 and 2, 875 p.

Dhital, M. R., Khanal, N. R., and Thapa, K. B., 1993, *The role of extreme weather events, mass movements and land use change in increasing natural hazards*: A report of the preliminary field assessment and workshop on causes and recent damage incurred in south central Nepal. 19–20 July 1993, ICIMOD, Kathmandu, 123+p.

ILWIS (The Integrated Land and Water Information System), 1997, User's Guide, ILWIS Department, International Institute for Aerospace Survey and Earth Science Enschede, The Netherlands. pp. 419–420.

Mehrotra, G. S., Sarkar, S., Kanungo, D. P., and Mahadevaiva, K., 1996, Terrain analysis and spatial Assessment of Hazards in parts of Sikkim Himalaya. Jour. of Geol. Soc. of India, v. 47, pp. 491–498.

Selby, M. J., 1993, *Hillslope material and processes*. Second edition, Oxford University Press, Oxford, 450p.

Starkel, L., 1972, The role of catastrophic rainfall in the shaping of the relief of the lower Himalaya (Darjeeling Hills). Geographia Polonica, v. 21, pp 103–147.

Stocking, M. A., 1972, Relief Analysis and Soil Erosion in Rhodesia Using Multivariate Techniques. Ztschrf. Geom., v. 16(4), pp. 432–433.

Survey Department, His Majesty's Government of Nepal, 1993, Topographic maps of Lumbini Zone, produced in cooperation with the Japan International Cooperation Agency (JICA), 6 sheets (098-05, 098-06, 098-07, 098-09, 098-10, 098-11).

UNDRO (Office of the United Nations Disaster Relief Co-ordinator), 1991, *Mitigation Natural Disasters: Phenomena, Effects and Options: A manual for Policy Makers and Planners*. United Nations, New York, 164 p.

Varnes, D. J., 1984, *Landslide hazard zonation: A review of principles and practices, Natural Hazards*. UNESCO, No. 3, 66 p.

Verstappen, H. Th., 1983, *Applied Geomorphology*. Elsevier Science Publishers B. V., Amsterdam, 437.

Van Westen, C. J., 1993, Slope Instability Recognition, analysis and Zonation. ITC, Jour., the Netherlands.